THE EFFECT OF VIRGIN COCONUT OIL CONTENT ON THE RHEOLOGICAL PROFILE OF VIRGIN COCONUT OIL-BASED LAMELLAR LIQUID CRYSTAL OF MIXED TWEEN 80:BRIJ 30 SYSTEM

Nor Ain Mohamed Arifin[1], Wan Rusmawati Wan Mahamod[1*], Norlaili Abu Bakar[1], Norhayati Hashim[1], Norzakiatul Husna Isnolamran[1] and Siti Aisyah Shamsudin[2]

[1]Department of Chemistry, Faculty of Science and Mathematics, Universiti Pendidikan Sultan Idris, 35900 Tanjung Malim, Perak, Malaysia
[2]Department of Applied Physics, Faculty of Science and Technology, Universiti Kebangsaan Malaysia, 43600 Bangi, Selangor, Malaysia

[*]rusmawati@fsmt.upsi.edu.my

Abstract. The health advantages of virgin coconut oil (VCO) and the diversity of its biological characteristics have garnered considerable attention recently. Nevertheless, scientific research on VCO-based applications is still under-reported particularly in Malaysia. This study aimed to investigate the effect of VCO content on the rheological profile of virgin coconut oil-based lamellar (V-Lα) liquid crystal systems of Tween80:Brij30/H_2O/VCO. In addition, the influence of mixed surfactant to water (MS/W) ratio also investigated. V-Lα samples formulated using the titration method. The formation of lamellar liquid crystals confirmed based on the existence of birefringence texture and the appearance of two recurring scattering peaks in the SAXS spectrum. The rheological study shows that V-Lα samples exhibit the shear-thinning behaviour of pseudoplastic materials with a yield stress range of 11.4 – 50.0 Pa. The effects of VCO content and MS/W ratio was mutually significant on rheological profiles of V-Lα. The pseudoplastic properties of the Lα structure increased with increasing VCO content for samples with lower MS/W (0.56/0.44) while the pseudoplastic properties weakened with increasing MS/W especially at high VCO (10 wt%) content. These rheological findings of the V-Lα will open greater application opportunities in industries, especially pharmaceuticals, because of the uniqueness of lamellar liquid crystals that can mimic lipid skin bilayers and the health benefit of VCO.

Keywords: Lamellar Liquid Crystal, Virgin Coconut Oil, Rheological Analysis, SAXS

Article Info

Received 10th October 2021
Accepted 22nd November 2021
Published 20 th December 2021

ISSN: 1823-7010, eISSN: 2600-7444

Introduction

Liquid crystal is a mesophase that maintains specific arrangement as crystal but flows like a liquid [1–3]. This phase had long-ranged orientational order that was mainly categorised into lyotropic and thermotropic [4]. The lyotropic liquid crystal induced by the addition of solvent is a multifunctional and versatile carrier because it enhances permeation ability [5]. Commonly, lyotropic liquid crystal was classified into lamellar (Lα) phase, hexagonal (H) phase and cubic (Q) phase [6]. Meanwhile, thermotropic liquid crystal formed by changes of temperature was popular in chemical sensor and electronic display application such as laptops and mobile phones [5].

The unique internal structure of Lα liquid crystal that is similar to the stratum corneum (SC) structure of living organisms has increased its potential applicability. Furthermore, the Lα phase has good compatibility with lipophilic and hydrophilic compounds [7]. System of Lα liquid crystal is made up of alternating layers of amphiphilic and hydrophilic water molecules [8–10]. Lα liquid crystal requires a solvent, such as water or oil, a surfactant and, if possible, a co-surfactant [3,11]. This system is classified as easily prepared and controlled [12,13]. However, in terms of suitability for applications, many factors will affect the system such as the type and amount of surfactant, the composition of components, stability of oil, pH, temperature, processing conditions and so on [14].

Virgin coconut oil (VCO) was reported to have a high level of oxidative stability compared with olive oil and sunflower oil [15]. Therefore, a formulation of V-Lα is highly proposed to enhance better skin penetration as oil alone has difficulty permeating the skin. VCO is extracted naturally without the use of chemicals from fresh and matured coconut kernels [16,17]. VCO is composed of triglyceride that are high in medium chain fatty acid (MCFA) such as lauric acid, followed by myrictic acid, palmitic acid, caprylic acid, capric acid, oleic acid, stearic acid, linoleic acid and caproic acid, with present of phenolic acid [18]. These chemical compositions of VCO have exhibit an excellent therapeutic effect [19]. VCO was formerly considered the healthiest oil globally due to its anti-inflammatory, antimicrobial, antioxidant, and anticancer properties [15,18,20]. Previous studies on topical application of VCO show that this oil is safe and non-toxic because it is rich in biological properties. Thus, VCO has great potential especially in pharmaceutical applications [15,19,21]. However, inadequate scientific studies of rheological profile on VCO-based applications were reported in comparison to the benefits discussed.

The rheological profile was investigated to respond to the demand of an application by adjusting the ratios of the surfactant as well as the oil and aqueous phases [22,23]. This study anticipates that the developed systems with specific rheological properties would be implemented in specific applications. Therefore, in order to determine the potential of V-Lα, this study evaluated the influence of VCO contents on the rheological profile of V-Lα liquid crystal of Tween80:Brij30/H_2O/VCO system. Furthermore, the effect of the mixed surfactant to water (MS/W) ratio on the V-Lα application also investigated in this study. The texture and phase properties were distinguished using optical polarising microscopy (OPM) [24]. Lα phase typically exhibited black and white birefringence texture with oily streak textures and maltese crosses [24]. The existence of Lα phase was then confirmed using small-angle x-ray scattering (SAXS). Spectra with two recurrent scattering peaks and a scattering vector, q ratio of 1:2 indicate the Lα phase [2]. Meanwhile, rheological analysis comprised the flow properties and behavior of the V-Lα samples. A rheological profile that includes viscosity, flow type and elasticity is comprehensive and relevant to the topical application [25].

Materials and Methods

Materials. The non-ionic surfactant polyoxyethylene 4 lauryl ether (Brij 30) was supplied by Sigma-Aldrich, USA, while polysorbate 80 (Tween 80) was supplied by Across Organics, Belgium. Virgin coconut oil (VCO) purchased from Man VCO Enterprise, Malaysia. All of the compounds were utilised without further purification. All samples preparation using deionised water that had been double distilled.

Preparation of V-Lα samples. Tween80:Brij30/H_2O/VCO mixed surfactants system samples prepared using a titration method described in the previous phase diagram [26]. A 5-gram sample prepared at the desired composition in the test tube, as shown in Table 1. This study used two different mixed surfactant to water ratio (MS/W), Tween80:Brij30/H_2O of 0.56/0.44 and 0.63/0.37 with 5 wt% and 10 wt% VCO contents. Meanwhile, the Tween 80 to Brij 30 ratio fixed at 1:9. Firstly, a vortex mixer used to mix Brij 30 with VCO. Then, deionised water and Tween 80 added and mixed for 20 minutes with the vortex mixer. Before centrifuging the test tube at 3000 rpm to eliminate bubbles, parafilm used to seal the test tube to avoid evaporation and leakage. The samples left undisturbed for three days to allow formation of liquid crystalline structures.

Table 1. Composition of Tween80:Brij30/H_2O/VCO mixed surfactants system samples.

Composition / MS/W ratio	5 wt% VCO		10 wt% VCO	
	Surfactant, wt%	**Water, wt%**	**Surfactant, wt%**	**Water, wt%**
0.56/0.44	53.2	41.8	50.0	40.0
0.63/0.37	60.0	35.0	56.7	33.3

Optical polarising microscopy (OPM). LCs texture identified by optical polarising microscopy (Leica DM EP, Wetzlar, Germany). A small amount of sample put on a microscope slide. The coverslip promptly added to minimise evaporation and carefully pressed to achieve the desired thickness. Sample patterns examined with a 10x magnification. The images of LCs captured with a Nikon H550S optical camera and an exposure controller connected to the microscope. Then, the LC pattern was investigated.

Small-angle x-ray scattering (SAXS). The scattering pattern of the LCs observed using a small-angle x-ray scattering (SAXS) approach from SAXSpace (Anton Paar, Austria). The device equipped with an X-ray tube that produces Cu-K radiation (= 0.1542 nm) at 40kV and 50mA. The sample placed in a sample holder and put into an X-ray machine, with a sample detector distance (SDD) of 317 mm. The temperature set at 25.0°C. Then, SGI software used to determine the LC phases and the corresponding lattice parameter (Space Group Indexing, v.03.2012).

Rheological measurement. The rheological measurements performed with a PHYSICA MCR 301 rheometer (Anton Par, Germany) at a constant temperature of 25 ± 0.1°C. A cone-plate sensor (20 mm diameter, 1° angle) was utilised. . The plate slowly raised to its measuring position and then the sample inserted on top of the plate of the sensor in constant velocity. The excess sample from the sensor system carefully removed. Initially, all samples were run the oscillatory measurements (amplitude sweeps) at 1 Hz in order to define the linear viscoelastic area. The orientational behaviour of Lα liquid crystal dispersions under shear investigated using steady-state shear flow curves. RheoPlus software displayed the pattern of the amplitude sweep and flow curve of the liquid crystals.

Results and Discussion

Optical polarising microscopy. Table 2 shows the OPM images of V-Lα samples at different MS/W ratios and VCO content. A clear birefringence characteristic observed through the appearance of the entire OPM images. The birefringence texture with oily streak and maltese crosses are characteristics of the Lα phase [2,4,24]. The VCO content shows a significant effect on V-Lα samples with higher MS/W (0.63/0.37). The maltsese cross texture becomes more dominant with the addition of 10 wt% VCO. Meanwhile, the V-Lα samples with lower MS/W (0.56/0.44) imposed almost similar texture of Lα phase. On other hand, the effect of MS/W may be noticed when the texture of the maltese cross begins to appear between the oily streak textures at higher MS/W. This finding shows that when MS/W increases, the texture of Lα weakens. However, additional information provided in-depth through rheological analysis.

Table 2: OPM images of V-Lα samples of Tween80:Bij30/H_2O/VCO

MS/W	VCO content		
	5 wt%		10 wt%
0.56/0.44	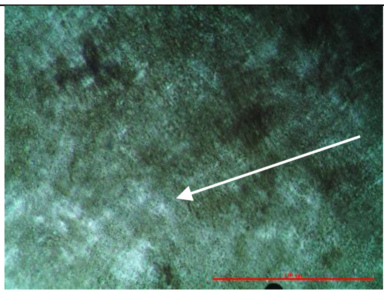	Oily streak	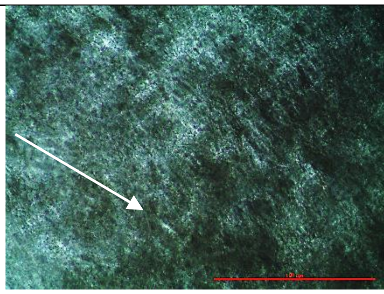
0.63/0.37	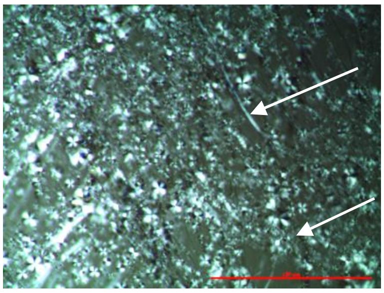	Oily streak Maltese cross	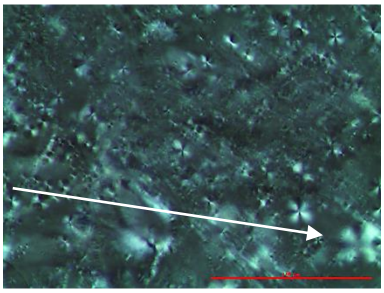

Small-angle X-ray scattering analysis. Based on the presence of maltese cross on the OPM image texture, SAXS analysis only conducted on V-Lα samples at an MS/W ratio of 0.63/0.37 for two different VCO contents, as shown in Figure 1. Spectra with two recurring scattering peaks, peak 1 and peak 2, in a ratio of scattering vector, q of 1: 2 appeared in both V-Lα samples of different VCO contents. SAXS analysis performed to confirm the presence of Lα texture in accordance with OPM analysis. These X-ray diffraction patterns is known as Lα phase characteristics [27]. The presence of Lα phase is consistent with the OPM observation. The result also shows that the scattering vector, q of first and second scattering peaks, shifted to a higher value as the oil content increased.

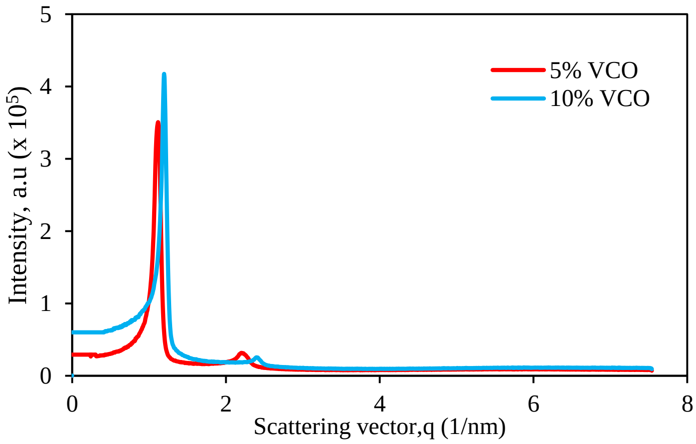

Figure 1. SAXS intensity profiles of V-Lα samples of Tween80:Brij30/H_2O/VCO at MS/W of 0.63/0.37.

In order to monitor the effect of the VCO content, the interlayer spacing, d of Lα calculated based on the average of d from $d=2\pi/q^1$ and $d=4\pi/q^2$ for the first and second-order of diffraction, respectively. Table 3 shows the values of interlayer spacing, where the values of d are 54.1 Å and 52.1 Å for V-Lα samples with 5 wt% VCO and 10 wt% VCO, respectively. The insignificant decrease in the d value of 2 Å is likely due to the existence of strong interactions between the hydrocarbon chains of surfactant molecules. The presence of up to 10 wt% VCO in the composition of V-Lα samples did not disturb the structure of Lα or in other words did not cause the lamellar layers to be swollen. These findings contrast those of Laili et al., (2017), who observed that as the oil content rose, so did the distance between layers. The discrepancy in these results might be attributed to the different surfactant types employed since this study used a non-ionic surfactant mixture. In contrast, Laili et al., (2017) used an mixture of anionic and cationic surfactants. Stearic hindrance did not occur in this study because the non-ionic surfactant did not generate any charges, meanwhile stearic hindrance by bulky anionic surfactants can push cationic molecules upwards and lead to an increase in the amphiphilic layer thickness [28].

Table 3. Interlayer spacing of lamellar, d for V-Lα samples of Tween80:Brij30 / H_2O / VCO at MS/W of 0.63/0.37

VCO content	Interlayer spacing of lamellar, d (Å)
5 wt%	54.1
10 wt%	52.1

Rheological analysis

Amplitude Sweep. Figure 2 demonstrates that the viscoelastic response of the V-Lα samples is comparable to that of the G' and G" which decreased concurrently beyond threshold as the shear strain increased. The amplitude sweep profiles consisting of storage modulus, G' and loss modulus, G" against the applied shear strain were conducted to determine the linear viscoelastic range (LVR). LVR provides information on the resilience of the material to applied strain/stress and tests can be performed without destroying the structure of the sample. The value of G' denotes the elasticity property whereas G" denotes the viscosity property. The fact that value of G' is greater than G" before the crossover point and value of G" is greater than G' after the crossover point clearly defines the typical characteristic of a gel-like rheogram [25].

The rheological parameter of limiting value of LVR, value of G' and tan δ (= G"/G') at 0.01% strain, G' and strain at the crossover point for Lα phases are presented in Table 3. Regardless of VCO content, the limiting value of LVR for the V-Lα samples remained at 0.8% for MS/W of 0.56/0.44 and 0.6% for MS/W of 0.63/0.37. The effects of VCO content and MS/W was mutually significant on rheological profiles of the V-Lα samples. The VCO content had a significant effect on the rheological profile of the V-Lα samples with higher MS/W compared to lower MS/W, where it can be seen from the significant changes in tan δ and G' values (at 0.01% strain and crossover point). A significant increase in the value of tan δ and a decrease in the value of G' with the addition of 10 wt% VCO indicates that the Lα structure is getting weaker. Meanwhile, for lower MS/W, almost consistent tan δ and strain (at crossover point) values indicate that the Lα structure of samples is more resistant to VCO addition. At fixed VCO content, increased MS/W affected the rheological profile of V-Lα samples where more significant changes occurred at a low VCO content (5 wt%). G' and tan δ decreased drastically from 900 Pa to 676 Pa and 0.18 to 0.14, respectively, with an increase in MS/W at 5 wt% VCO. The decrease in tan δ is due to the decrease in G" relatively parallel to the curve G'. This indicates that the pseudoplastic properties of the V-Lα samples remained strong despite a decrease in the elastic properties of the samples. A better and more explicit confirmation of changes in the pseudoplastic properties of V-Lα samples can be obtained from frequency sweep and flow curve tests. In this study, we only conducted flow curve tests to confirm changes in pseudoplastic properties.

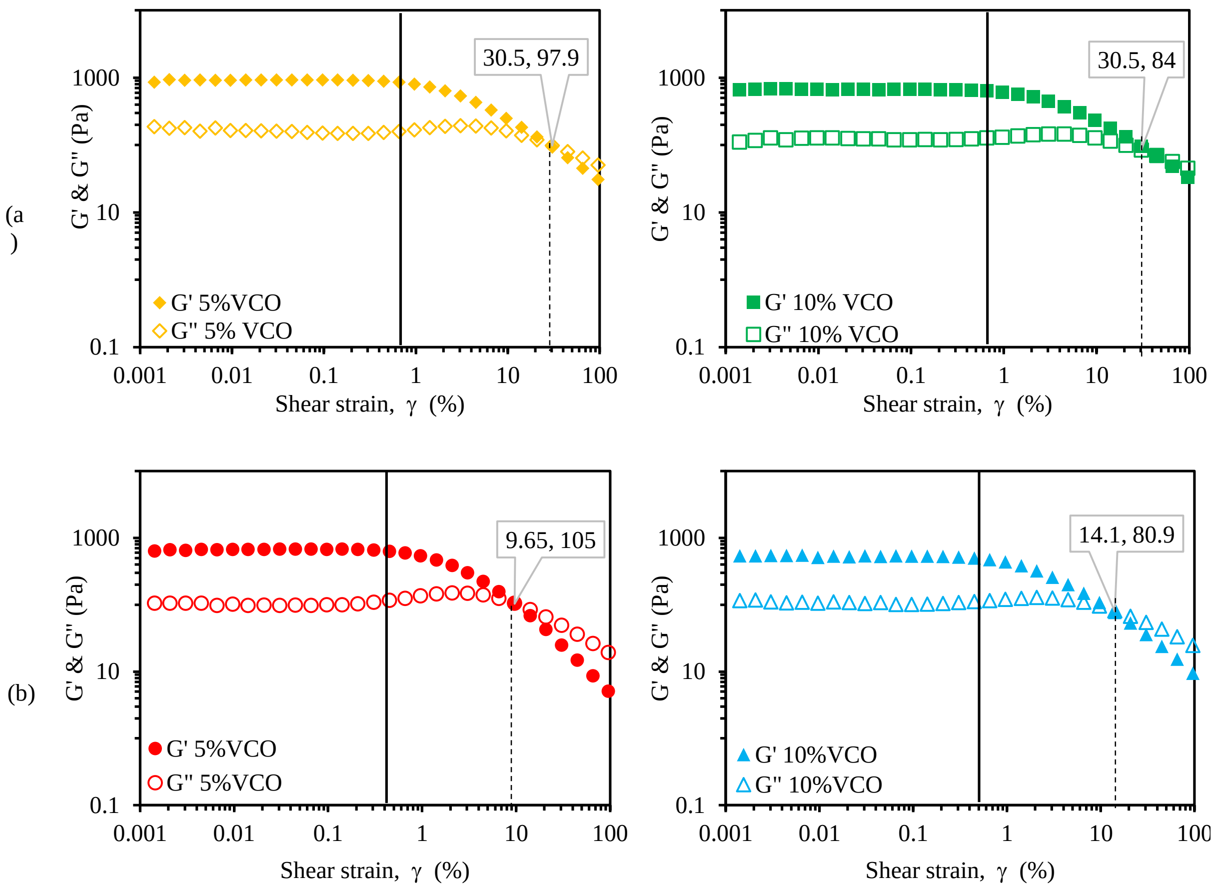

Figure 2. Amplitude sweep profiles of V-Lα samples of Tween80:Brij30/H_2O/VCO with (a) MS/W 0.56/0.44 and (b) 0.63/0.37 of different VCO content

Table 3. Rheological parameters of amplitude sweep profiles for V-Lα samples of Tween80:Brij30/H_2O/VCO

Parameters / MS/W ratio	VCO content	Limiting value of LVR (%)	Value at 0.01% strain		Crossover point at G'= G"	
			G' (Pa)	tan δ	G' (Pa)	Strain (%)
0.56/0.44	5 wt%	0.8	921	0.18	97.9	30.50
	10 wt%	0.8	665	0.19	84.0	30.50
0.63/0.37	5 wt%	0.6	676	0.14	105.0	9.65
	10 wt%	0.6	533	0.21	80.9	14.10
LVR: linear viscoelastic range, G': storage modulus						

Flow curve. Figure 3 depicts the common shear-thinning flow behaviour by rising viscosity as the shear rate approaches zero and a proportionate rise in shear stress as a function of shear rate. These flow responses of Tween80:Brij30/H_2O/VCO system show a shear-thinning behavior with a yield stress, τ_0, also known as pseudoplastic flow [29]. Table 4 shows the rheological parameters of the power-law index -(n-1) for three distinct shear rate ranges, <1s $^{-1}$, 1-100s^{-1} and 100-1000s^{-1}. According to the previous study, flow behaviour can be represented by power-law shear-thinning models, $\eta = K_{\gamma}^{-(n-1)}$ [27]. The -(n-1) value represents the organization of the Lα phase structure [27]. The power-law values of all V-Lα samples approaching -1 (Table 4) at low shear rates, regardless of VCO content, exhibit the shear-thinning behavior of the pseudoplastic material [29,30]. This value illustrates that the Lα network is connected continuously and in parallel. The values also suggest that the sliding effect between bilayer structures is common under shear. The V-Lα samples shared the same behaviour, as they did not flow until they reached the stress limit point, yield stress. The decrease in power-law values with increasing shear rate indicates the ability of the Lα phase to form dense layered structure [31].

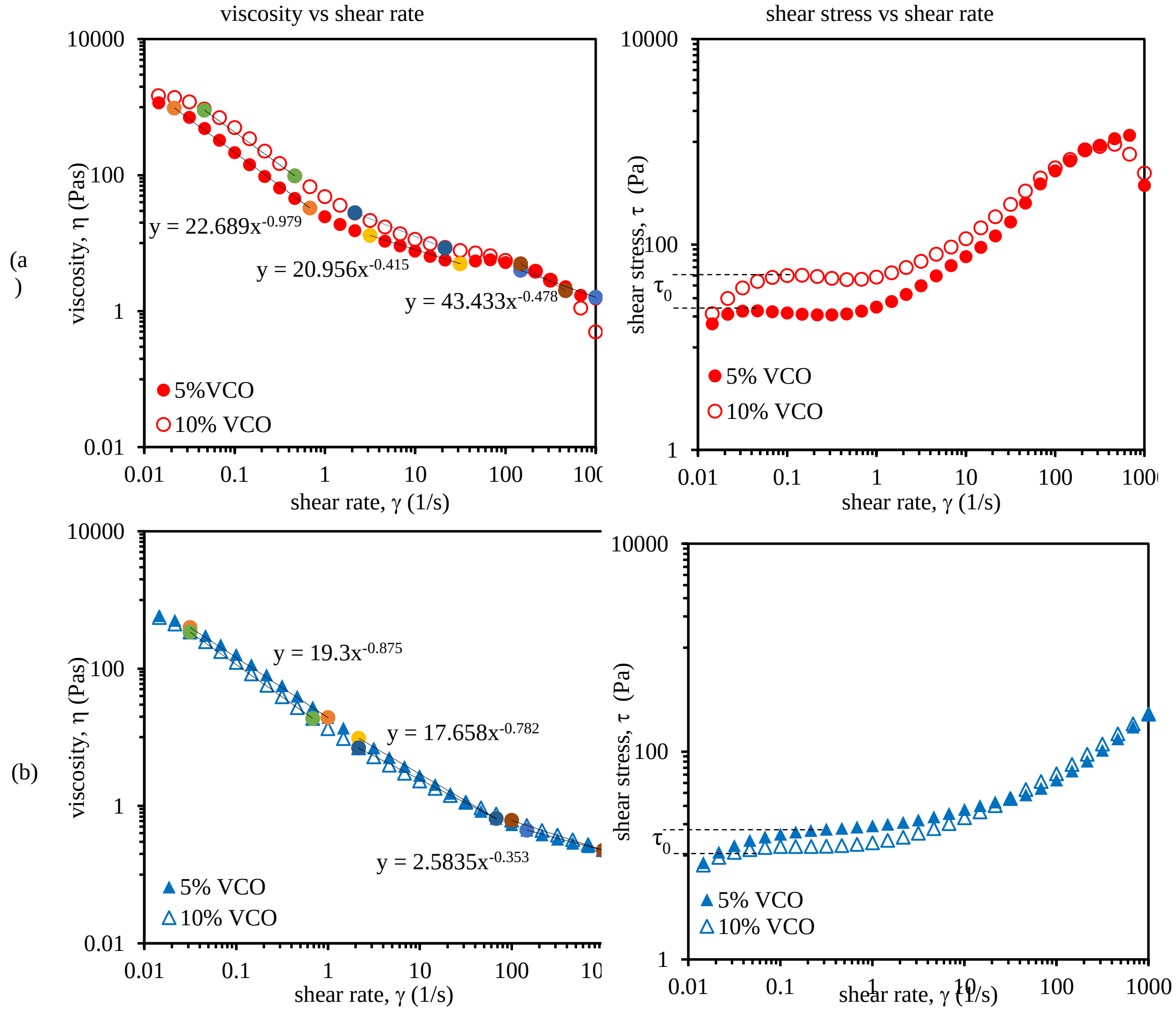

Figure 3. Flow curve profiles of V-Lα samples of Tween80:Brij30/H_2O/VCO with (a) MS/W 0.56/0.44 and (b) 0.63/0.37 of different VCO content

Table 4. Rheological parameters of flow curve profiles for V-Lα samples of Tween80:Brij30/H_2O/VCO

Parameters / MS/W ratio	VCO content	-(n-1)			Viscosity, η at 1 s^{-1} (Pas)	Yield Stress, τ_0 (Pa)
		< 1 s^{-1}	1-100 s^{-1}	100-1000 s^{-1}		
0.56/0.44	5 wt%	-0.979	-0.415	-0.478	24.5	22.6
	10 wt%	-0.965	-0.518	-0.797	48.3	50.0
0.63/0.37	5 wt%	-0.875	-0.782	-0.353	19.3	17.9
	10 wt%	-0.941	-0.687	-0.436	13.3	11.4

The flow curve also shows that the increase in VCO content at fixed MS/W influences the viscosity characteristics of the sample where the V-Lα samples shows a more significant effect at low MS/W. The addition of VCO content is able to modify the shear thinning behavior (power-law value change from -0.478 to -0.797 s^{-1}) at a high shear rate range, illustrating the strengthening of Lα structure that also can be seen from the increase in yield stress value by two times. This clearly indicates that the increase in VCO to V-Lα samples with low MS/W strongly influenced the pseudoplastic properties of the Lα structure, although the amplitude sweep results did not have a significant effect (tan δ values were almost consistent). When MS/W increased at fixed VCO, notably at 10 wt%, the Lα structure shown to weaken based on a drastic decrease in power-law (-0.797 to -0.436) at high shear range and yield stress (50.0 to 11.4 Pa) values. This phenomenon is parallel to the results obtained from the amplitude sweep test. The results showed that the pseudoplastic properties of the Lα structure increased with increasing VCO content for samples with low MS/W, while the pseudoplastic properties weakened with increasing MS/W, especially at high VCO content.

Based on the rheological parameters, it can be concluded that the Lα structure of the V-Lα sample at a low MS/W ratio is the strongest. The addition of a VCO of up to 10 wt% between the surfactant hydrocarbon chains further strengthens the Lα structure through hydrocarbon interactions. The increase in MS/W ratio relatively increases the content of Brij 30 in the surfactant mixture which is more hydrophobic and more oriented towards the hydrophobic moiety of the VCO. This causes the interaction between surfactant molecules in the interstitial layer to weaken and in turn, weakens the structure of V-Lα sample [32].

Conclusion

In this study, VCO-based Lα (V-Lα) samples that display the shear-thinning behaviour of pseudoplastic materials were effectively formulated and characterised. Both factors, VCO content and ratio of MS/W play their respective roles in influencing the rheological profile of Lα structures. The pseudoplastic properties of the Lα structure increased with increasing VCO content for V-Lα samples with lower MS/W (0.56/0.44), while the pseudoplastic properties weakened with increasing MS/W, especially at high VCO (10 wt%) content. In conclusion, V-Lα samples with MS/W 0.56/0.44 of the Tween80:Brij30/H_2O/VCO system possess a better rheological profile than M/SW 0.63/0.37. Due to the sheer distinctiveness of lamellar liquid crystals that may replicate lipid skin bilayers to boost active ingredient penetration and health benefit of VCO, this rheological profile of the V-Lα study offer more application, particularly pharmaceutical. As a result, additional research into this composition and method is recommended.

Acknowledgements

The Malaysian Ministry of Education funded this study under the Fundamental Research Grants Scheme (FRGS/1/2018/STG01/UPSI/02/7). The authors would like to thank Universiti Pendidikan Sultan Idris (UPSI) for assisting with grant management.

Author Contributions

All authors contributed toward data analysis, drafting and critically revising the paper and agree to be accountable for all aspects of the work.

Disclosure of Conflict of Interest

The authors have no disclosures to declare.

Compliance with Ethical Standards

The work is compliant with ethical standards.

References

[1] Ashok, C. K., Ola, M. M., Ramesh, D. R., & Ashok, V. (2019). Liquid crystals: A review. *Int. J. Creat. Innov. Res. All Stud* 1, 119–129

[2] Salimin, N. R., Mahamod, W. R. W., Bakar, N. A., Azziz, S. S. S. A., Sharif, A. M., Pauzan, N. A., & Hashim, N. (2019). Characterisation of virgin coconut oil based lamellar liquid crystal incorporated with lycopene. *Journal of Advanced Research in Dynamical and Control Systems*, 11(Special Issue 6) 1852–1858.

[3] Laili, C. R., Hamdan, S., Azhar, M. S., & Hasham, R. (2017). Molecular arrangement of lamellar liquid crystalline structure with virgin coconut oil. *Asian Journal of Chemistry*, 29(10) 2129–2132.

[4] Milak, S., & Zimmer, A. (2015). Glycerol monooleate liquid crystalline phases used in drug delivery systems. *International Journal of Pharmaceutics*, 478(2) 569–587.

[5] Madheswaran, T., Kandasamy, M., Bose, R. J., & Karuppagounder, V. (2019). Current potential and challenges in the advances of liquid crystalline nanoparticles as drug delivery systems. *Drug Discovery Today*, 24(7) 1405–1412.

[6] Wang, D., Cao, Y., Cao, M., Sun, Y., Wang, J., & Hao, J. (2016). Dual-responsive viscoelastic Lyotropic liquid crystal fluids to control the diffusion of hydrophilic and hydrophobic molecules. *ChemPhysChem*, 17(13) 2079-2087.

[7] Salmazi, R. (2015). A curcumin-loaded liquid crystal precursor mucoadhesive system for the treatment of vaginal candidiasis. *International Journal of Nanomedicine,* 4815–4824.

[8] Da Rocha-Filho, P. A., Maruno, M., Ferrari, M., & Fernando Topan, J. (2016). Liquid crystal formation from sunflower oil: Long term stability studies. *Molecules*, 21(6) 1–16.

[9] Rapalli, V. K., Waghule, T., Hans, N., Mahmood, A., Gorantla, S., Dubey, S. K., & Singhvi, G. (2020). Insights of lyotropic liquid crystals in topical drug delivery for targeting various skin disorders. *Journal of Molecular Liquids*, 315 113771.

[10] Huang, Y., & Gui, S. (2018). Factors affecting the structure of lyotropic liquid crystals and the correlation between structure and drug diffusion. *RSC Advances*, 8(13) 6978–6987.

[11] Wang, X., Zhang, Y., Gui, S., Huang, J., Cao, J., Li, Z., Li, Q., & Chu, X. (2018). Characterization of Lipid-Based Lyotropic Liquid Crystal and Effects of Guest Molecules on Its Microstructure: a Systematic Review. *AAPS PharmSciTech*, 19(5) 2023–2040.

[12] Rajabalaya, R., Musa, M. N., Kifli, N., & David, S. R. (2017). Oral and transdermal drug delivery systems: Role of lipid-based lyotropic liquid crystals. *Drug Design, Development and Therapy*, 11 393–406.

[13] Oyafuso, Márcia H., Carvalho, F. C., Takeshita, T. M., de Souza, A. L. R., Araújo, D. R., Merino, V., Gremião, M. P. D., & Chorilli, M. (2017). Development and in vitro evaluation of lyotropic liquid crystals for the controlled release of dexamethasone. *Polymers*, 9(8) 1–16.

[14] McClements, D. J., & Jafari, S. M. (2018). Improving emulsion formation, stability and performance using mixed emulsifiers: A review. *Advances in Colloid and Interface Science*, 251 55–79.

[15] Aqilah, N., Channip, A. G. A., Chok, P., Hwa, H., Ja, F., & Anwar, M. Y. (2018). Physicochemical properties , antioxidant capacities , and metal contents of virgin coconut oil produced by wet and dry processes. *Food Sci Nutr,* 6(5) 1298-1306.

[16] Varma, S. R., Sivaprakasam, T. O., Arumugam, I., Dilip, N., Raghuraman, M., Pavan, K., Rafiq, M., & Paramesh, R. (2019). In vitro anti-inflammatory and skin protective properties of virgin coconut oil. *Journal of Traditional and Complementary Medicine*, 9(1) 5-14.

[17] Srivastava, Y., Semwal, A. D., Sajeevkumar, V. A., & Sharma, G. K. (2017). Melting, crystallization and storage stability of virgin coconut oil and its blends by differential scanning calorimetry (DSC) and Fourier transform infrared spectroscopy (FTIR). *Journal of Food Science and Technology*, 54(1) 45–54.

[18] Illam, S. P., Narayanankutty, A., & Raghavamenon, A. C. (2017). Polyphenols of virgin

coconut oil prevent pro-oxidant mediated cell death. *Toxicology Mechanisms and Methods*, 27(6) 442–450.

[19] Chew, Y. L. (2019). The beneficial properties of virgin coconut oil in management of atopic dermatitis. *Pharmacognosy Reviews*, 13(25) 24.

[20] Imelda, Lister, I. N., Fachrial, E., Ginting, C. N., & Lie, S. (2020). An experiment of virgin coconut oil treatments for burn incidence on rabbits. *2020 3rd International Conference on Mechanical, Electronics, Computer, and Industrial Technology (MECnIT)*, pp. 386-389

[21] Zicker, M. C., Silveira, A. L., Lacerda, D. R., Rodrigues, D. F., Oliveira, C. T., De Souza Cordeiro, L. M., Lima, L. C., Santos, S. H., Teixeira, M. M., & Ferreira, A. V. (2019). Virgin coconut oil is effective to treat metabolic and inflammatory dysfunction induced by high refined carbohydrate-containing diet in mice. *The Journal of Nutritional Biochemistry*, 63 117-128.

[22] Chen, Y., Liang, X., Ma, P., Tao, Y., Wu, X., Wu, X., Chu, X., & Gui, S. (2015). Phytantriol-Based In Situ Liquid Crystals with Long-Term Release for Intra-articular Administration. *AAPS PharmSciTech*, 16(4) 846–854.

[23] Oyafuso, M. H., Carvalho, F. C., Chiavacci, L. A., Gremião, M. P., & Chorilli, M. (2015). Design and characterization of silicone and surfactant based systems for topical drug delivery. *Journal of Nanoscience and Nanotechnology*, 15(1) 817-826.

[24] Nalone, L., Marques, C., Costa, S., Souto, E. B., & Severino, P. (2020). Liquid crystalline drug delivery systems. In *Drug Delivery Trends*. (Elsevier Inc.)

[25] Silva, S. A. M. e., Lacerda, R., Bernegossi, J., Chorilli, M., & Leonardi, G. R. (2016). Development of nanotechnology-based drug delivery systems with olive vegetable oil for cutaneous application. *Brazilian Journal of Pharmaceutical Sciences*, 52(1) 211–219.

[26] Norhadisah MZ. (2012). *Phase Diagrams of Single Brij 30 Or Tweens Series (T20, T60, T80)/Water/VCO And Mixed Brij 30: Tween Series (T20, T60,T80)/Water/VCO System*. Universiti Pendidikan Sultan Idris, Perak, Malaysia

[27] Li, Z., Zhao, X., & Wang, Z. (2017). Study on the formation and rheological properties of sucrose stearate lamellar liquid crystals. *Journal of Dispersion Science and Technology*, 38(1) 152–158.

[28] Zhang, Z., Yang, H., Bi, J., Zhang, A., Fang, Y., Feng, Y., An, L., Liang, L., Zhang, C., & Pu, J. (2018). The leading role of the steric hindrance effect and dipole-dipole interaction in superlattice nanostructures formed via the assembly of discotic liquid crystals. *New Journal of Chemistry*, 42(24), 20087–20094.

[29] Rajak, P., Nath, L. K., & Bhuyan, B. (2019). Liquid crystals: An approach in drug delivery. *Indian Journal of Pharmaceutical Sciences*, 81(1) 11–23.

[30] Zuzanna, T. (2016). Rheology of printing inks. *Printing on Polymers.* (William Andrew) pp. 87-99.

[31] Akbari, S., & Nour, A. H. (2020). Emulsion types, stability mechanisms and rheology: A review. *International Journal of Innovative Research and Scientific Studies*, 1(1) 11-17.

[32] Ja'Afar, S. M., Khalid, R. M., Othaman, R., Mokhtar, W. N. A. W., & Ramli, S. (2019). Coconut oil based microemulsion formulations for hair care product application. *Sains Malaysiana*, 48(3) 599–605.